Optical properties of guanidinium aluminium sulphate hexahydrate (GASH)

1993 J. Phys.: Condens. Matter 5 3039

(http://iopscience.iop.org/0953-8984/5/18/026)

J. Phys.: Condens. Matter 5 (1993) 3039–3048. Printed in the UK

Optical properties of guanidinium aluminium sulphate hexahydrate (GASH)

P M Nikolic†, W B Roys†, X Maričić‡, G A Gledhill§, S Duric‡, G Radukić¶, V Radišić‡, P Mihajlovic‡, D M Todorović‡ and D Vasiljević‡

† Department of Physics, Nottingham University, UK
‡ Joint Laboratory for Advanced Materials of SASA (Serbian Academy of Sciences and Arts), 11000 Beograd, PO Box 366, Yugoslavia
§ Royal Holloway University of London, Egham, Surrey, UK
¶ Mining and Geology Faculty, Belgrade University, Yugoslavia

Received 8 August 1992, in final form 26 February 1993

Abstract. Far-infrared reflection spectra were determined, for the first time, for single crystals of guanidinium aluminium sulphate hexahydrate (GASH) and its solid solution for 5 mol% chromium isomorph (GCSH). The infrared active transversal and associated longitudinal phonon frequency and the dielectric permittivity functions for $E \parallel C$ and $E \perp C$ have been determined using both Kramers–Krönig analysis and a fitting procedure based on a four-parameter model. The indices of refraction were also measured using the immersion method with Cargille liquid and the results were compared with data obtained by numerical analysis of reflectivity measurements. The optical transmission of the samples were measured in the visible range and three wide energy bands were observed at about 2.6 eV, 3 eV and 4.9 eV for GASH doped with Cr, below the conduction energy zone.

1. Introduction

Guanidinium aluminium sulphate hexahydrate (GASH) $[C(NH_2)_3]Al(SO_4)_2{\cdot}6H_2O$ is a ferroelectric material with Curie temperature T_c = 743 K. It has a hexagonal lattice structure with space group $P31m$ (C_{3v}^2) with three molecules per unit cell. Schein *et al* [1] redetermined the crystal structure of GASH and obtained the following values for the lattice parameters: a_0 = 1.1738 ± 0.0002 nm and c_0 = 0.8951 ± 0.0002 nm. The spontaneous polarization, P_s, of GASH is similar to the value for Rochelle salt ($P_s \simeq 0.35 \times 10^{-6}$ C m^{-2} at 23 °C).

As far as we know, complete data on the optical and dielectric properties of GASH in the infrared (IR) and far-infrared (FIR) ranges have not been obtained for this relatively little known ferroelectric material.

In this work the optical properties of GASH samples were measured and analysed in the IR and FIR ranges and also in the absorption edge range. GASH samples were also doped with Cr and its influence on the optical properties of GASH is considered.

2. Experimental details

Single crystals of pure GASH were grown from an aqueous solution of guanidinium and aluminium sulphate. Single crystals of GASH doped with about 5 mol% Cr were made in the same way with addition of $Cr_2(SO_4)_3$. Pure GASH samples were transparent like glass,

0953-8984/93/183039+10$07.50

but samples doped with Cr were slightly blue. All single-crystal samples were hexagonally shaped plates.

The crystal structure and lattice parameters of the samples were determined using x-ray diffraction. The lattice parameters of pure GASH and GASH doped with Cr were calculated using powder diffractograms obtained by a Philips PW 1130 system with a copper-radiation tube and a curved graphite crystal monochromator. The goniometer had been previously calibrated with a high purity Si standard (PW).

The accuracy of our standard unity volume cell was better than that proposed by the International Union for Crystallography, i.e. our parameter for the Si standard was $a_0 = 0.54306 \pm 0.000006$ nm at 25 °C and the International Union Crystal Standard for Si is $a_0 = 0.543054 \pm 0.000017$ nm. We measured 51 reflections for pure GASH samples and 38 for GASH doped with Cr. All observed reflections of $K\alpha$ as well as separated $K\alpha_1$ and $K\alpha_2$, were used to calculate the lattice parameter using the least squares method. The results obtained for pure and doped GASH samples together with data available in the literature for pure GASH and GCSH crystals obtained by Schein *et al* [1] are given in table 1. V_0 is the volume of the unit cell. Its value was calculated using the relation $V_0 = a_0^2 c_0 \cos 30°$ for the hexagonal GASH lattice. The reason for giving this was that there were some differences between the values of the lattice parameters a_0 and c_0 obtained in this work and those given by Schein [1]. In this case it is better to give the value of the volume of the unit cell (V_0). There is a noticeable difference between our data and those given in the literature for pure GASH. This difference can be attributed to the smaller number of Bragg reflections used by Schein and co-workers. (They used 9 reflections compared with our 51.)

Table 1. The hexagonal unit cell parameters of GASH, GCSH and G(Al, Cr)SH.

	GASH	G(Al, Cr)SH	GASH[1]	GCSH[1]
a_0 (nm)	1.1731(3)	1.1739(2)	1.1738(2)	1.1754(3)
c_0 (nm)	0.8945(3)	0.8953(2)	0.8951(2)	0.9041(3)
V_0 (nm^3)	1.0660(7)	1.0686(5)	1.0681	1.0817

The samples suitable for reflectivity measurements were cleaved and all cleaved plates were parallel to the c plane (001). Pure GASH samples and those doped with Cr were hexagonally shaped plates with (001) orientation. These plates had rather large flat surfaces suitable for reflectivity measurements, with areas between 1 and 10 cm^2. The samples were between 2 and 5 mm in thickness; therefore it was very easy to measure reflectivity in the $\boldsymbol{E} \perp \boldsymbol{C}$ direction. In contrast reflectivity measurements in the $\boldsymbol{E} \parallel \boldsymbol{C}$ direction of the hexagonal plates were very difficult because the samples were thin and the measurements were done using several samples stuck together and then polished. In that case the thickness achieved was about 8 mm which was sufficient for the reflectivity measurements. Nevertheless, the polished surface was inferior to that of the (001) plate, so the intensity of the measured reflectivity was smaller than the values obtained for the $\boldsymbol{E} \perp \boldsymbol{C}$ direction. Normally incident light was assumed for all reflectivity measurements although the experimental angle was about 82°, because of the reflectivity adapters used.

Far-infrared reflectivity measurements were made with near-normal-incidence polarized light in the range 50 to 2500 cm^{-1} using a Grubb–Parsons/NPL FT interferometer and a Brucker 113V FTIR spectrometer. The resolution of the measurements was better than 1 cm^{-1}. The measurements for each sample were repeated several times and we always obtained practically the same results. The number of scans during these measurements was between 100 and 1000; therefore the signal-to-noise ratio for the sample and the reference

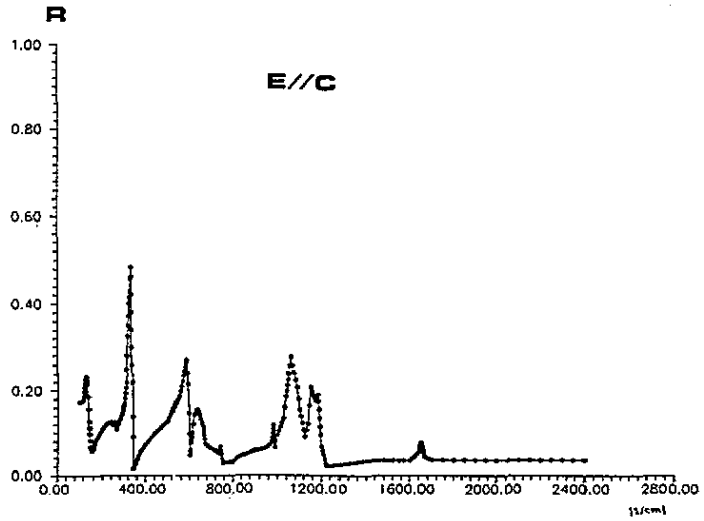

Figure 1. Room temperature reflectivity curve of GASH for $E \parallel C$ as a function of wave number. Spectral resolutions 1 cm^{-1}. The resolution of reflectivity measurements was better than 1%.

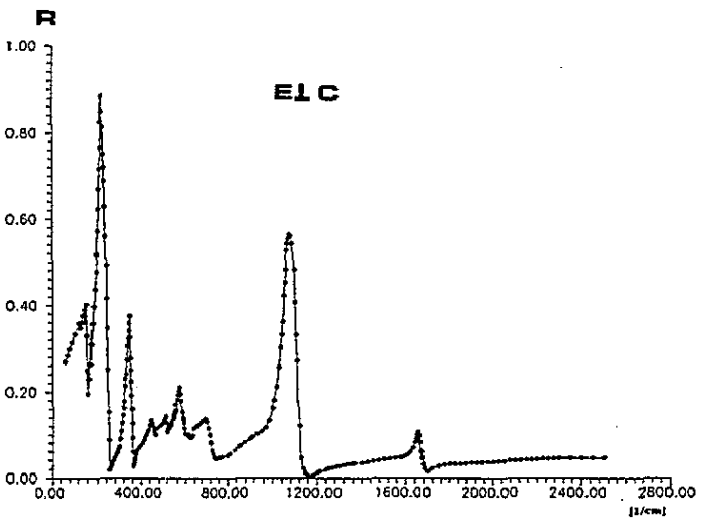

Figure 2. Room temperature curve of GASH for $E \perp C$ as a function of wave number. Spectral resolutions 1 cm^{-1}. The resolution of reflectivity measurements was better than 1%.

mirror allowed us to conclude that the precision of the reflectivity measurements was better than 1%.

Room temperature experimental reflectivity curves as a function of wave numbers in the infrared and far-infrared ranges are given for $E \parallel C$ and $E \perp C$ in figures 1 and 2, respectively. The experimental results are shown with dots while the full curves were calculated using Kramers–Krönig analysis. The error bars are of the size of the experimental points given in figures 1 and 2 due to good resolution of the reflectivity measurements (better than 1%).

A total of 11 oscillators polarized for $E \parallel C$ and 12 oscillators for the $E \perp C$ direction

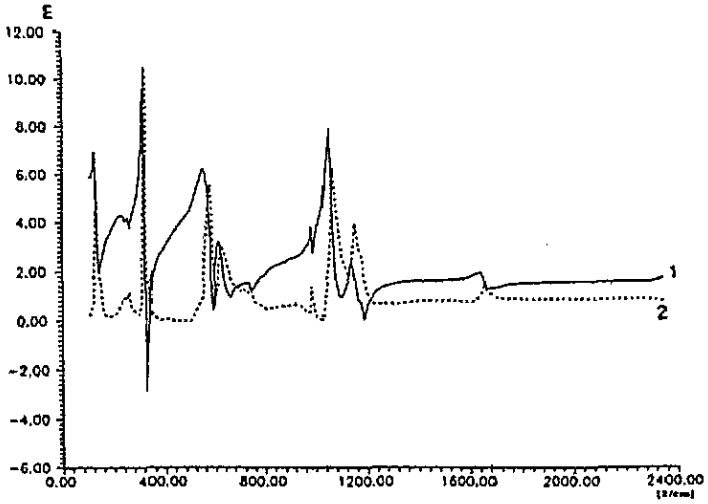

Figure 3. Variation of the real (ϵ_1) and imaginary (ϵ_2) parts of the complex dielectric function for $E \parallel C$. Solid curve ϵ_1; dashed curve ϵ_2.

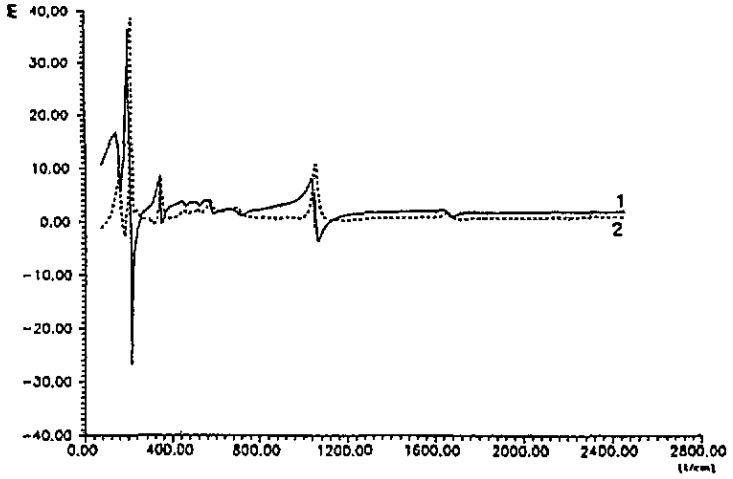

Figure 4. Variation of the ϵ_1 and ϵ_2 for $E \perp C$. Solid curve ϵ_1; dashed curve ϵ_2.

were observed. The diagrams of the real (ϵ_1) and imaginary (ϵ_2) parts of the complex dielectrical function are given in figures 3 and 4 for $E \parallel C$ and $E \perp C$ respectively. The accuracy of the instruments used for the reflectivity measurements was better than 1% and the uncertainties of the results obtained for both directions ($E \perp C$ and $E \parallel C$), for our available samples, were less than 1%. The quality of the surface for $E \perp C$ measurements was almost perfect because it was obtained by a cleavage procedure. The quality of the surface used for $E \parallel C$ measurements was poorer because it was obtained by a polishing procedure. The polishing procedure cannot give as good a surface as that obtained by cleavage. The polished surface shows a reflectivity coefficient up to 10% smaller than the reflectivity of a perfectly cleaved surface of the same material. In both cases we obtained

mirror-like surfaces which were used for the measurements. Since we think our level of reflectivity for $E \parallel C$, at the most pessimistic judgment, is up to 10% smaller than the maximum, the uncertainties of ϵ_1 and ϵ_2 in figures 4 and 3 should be less than 1% and 10%, respectively. The uncertainties of the positions of peaks given in figure 1, 2, 3 and 4 were less than 1 cm^{-1}.

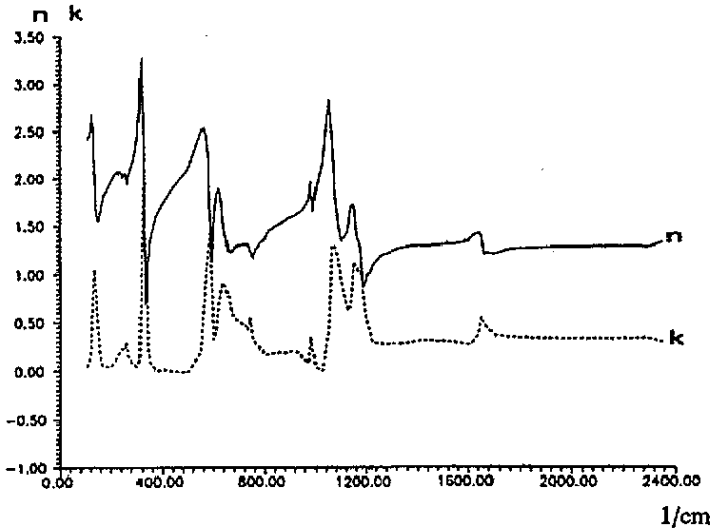

Figure 5. The refractive index (with full lines) and extinction coefficient (with broken lines) for $E \parallel C$.

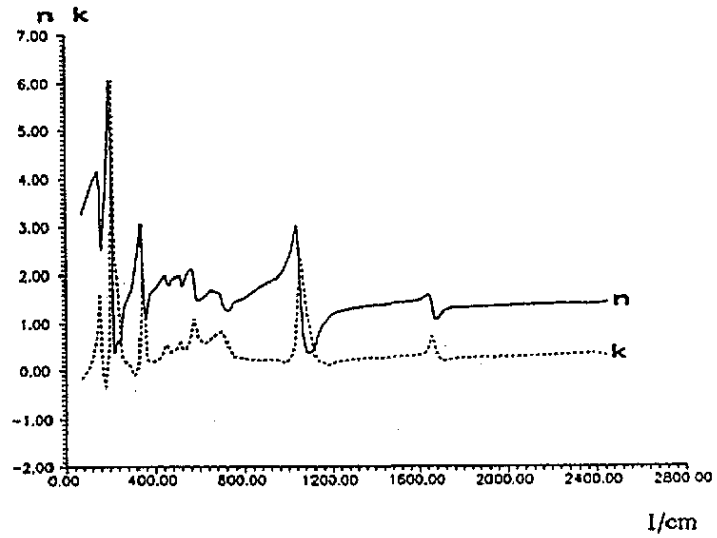

Figure 6. The refractive index (with full lines) and extinction coefficient (with broken lines) for $E \perp C$.

Figures 5 and 6 show the refractive indices (with full lines) and extinction coefficients (with broken lines) in the FIR range for $E \parallel C$ and $E \perp C$, respectively. The response function $\mathrm{Im}(-1/\epsilon)$ for $E \parallel C$ and $E \perp C$ is given in figures 7 and 8, respectively. Phonon

frequencies deduced from Kramers–Krönig analysis are shown in table 2 together with the phonon mode assignments based on the space group C_{3V}^2 and Wyckoff's sites of atoms (where ω_{jTO} and ω_{jLO} are transverse (TO) and longitudinal (LO) frequencies) and ϵ_0 and ϵ_∞ represent the low and high frequency contribution to the dielectric parameters. The parameter ω_{TO} was deduced from peaks of the imaginary part of the dielectric function (ϵ_2) and ω_{LO} from peaks of the response function $\mathrm{Im}(-1/\epsilon)$. The total number of active infrared modes was obtained using Adams–Newton tables 3:

$$\Gamma = 37\ \mathrm{A}_1 + 65\ \mathrm{E} \tag{1}$$

comprising 37 A_1 for $\boldsymbol{E} \parallel \boldsymbol{C}$ and 65 E for $\boldsymbol{E} \perp \boldsymbol{E}$. In this case we experimentally observed 26 oscillators less for $\boldsymbol{E} \parallel \boldsymbol{C}$ and 53 less for $\boldsymbol{E} \perp \boldsymbol{C}$.

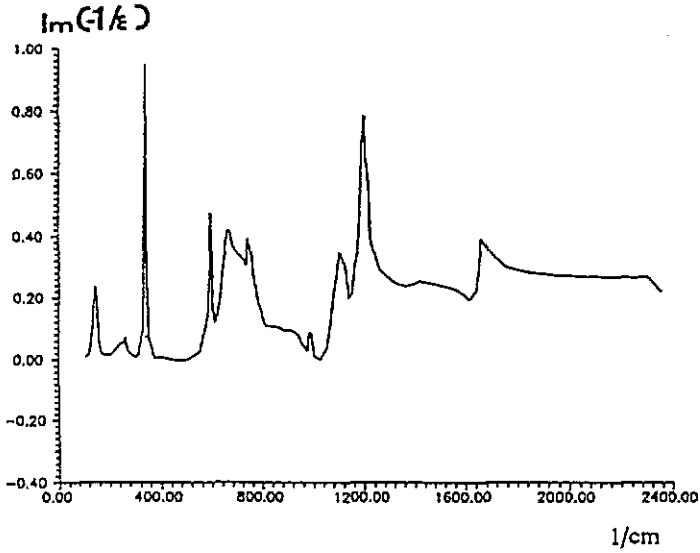

Figure 7. The response function $\mathrm{Im}(-1/\epsilon)$ for $\boldsymbol{E} \parallel \boldsymbol{C}$.

The optical transmission was measured in the range of the absorption edge using a Perkin–Elmer Lambda 5 spectrophotometer in the direction $\boldsymbol{E} \parallel \boldsymbol{C}$. The samples were 5 mm thick. The experimental results are given in figure 9(*a*) for pure GASH and in figure 9(*b*) for the GASH sample doped with Cr. The pure single-crystal GASH sample was transparent and this transparency was almost constant for wavelengths higher than the absorption edge range. GASH doped with Cr showed three absorbing energy bands: at approximately 2.6 eV, 3 eV and finally at about 4.8 eV, below the conduction energy band.

The indices of refraction were measured for both samples using a polarized microscope (Reichert) and the immersion method with Cargille liquid. These measurements were made at 23 °C with monochromatic Na light. The results obtained for both pure GASH and Cr-doped samples were very similar and they are given in table 3.

3. Discussion

In this work we initially redefined the lattice parameters of GASH to a greater accuracy than achieved previously.

Table 2. Phonon frequencies (in cm^{-1}) deduced from (a) Kramers–Krönig analyses and (b) the four-parameter model.

	(a)					(b)					
	ϵ_0	ϵ_∞		ω_{TO}	ω_{LO}	ω_{TO}	ω_{LO}	γ_{TO}	γ_{LO}	ϵ_0	ϵ_∞
$E \parallel C$	5.8	1.7	1	122	145	122.6	145.5	223.9	9.9	5.8	2.535
			2	230	245	231.5	246.5	73.6	126.3		
			3	315	340	258.7	262.7	353.4	237.9		
						321	340.9	6.3	7.2		
			4	550	595	556.4	594.8	94.7	4.3		
			5	620	670	630.7	678.8	93.6	171.7		
			6	731	752	724.2	774.6	334.8	278.4		
			7	981	981.5	992.4	993.4	78.4	31.2		
			8	1050	1100	1064.4	1127	55.2	48.4		
			9	1138	1196	1156.2	1194.6	35.6	35.6		
			10	1400	1410	1189.3	1205.6	59.6	194		
			11	1640	1660	1644.2	1667.6	168.9	232.5		
$E \perp C$	21.8	1.8	1	142	154	142	159.5	17.4	22.7	21.5	2.658
			2	200	243	201	241.8	2.12	20.5		
			3	330	350	336	351.5	15.9	12.8		
			4	400	415	413.5	415.5	63.2	64.8		
			5	430	454	447.7	453.3	33.7	35.8		
			6	472	492	—	—	—	—		
			7	500	515	514.1	518.7	30.5	25.7		
			8	531	588	562.7	592.6	48.7	50.3		
			9	627	735	684.7	726.6	75.5	92.7		
			10	875	888	890.7	893	40	46.3		
			11	1020	1128	1051	1116.2	28.7	22.3		
			12	1633	1673	1660.4	1675	35.7	35.9		

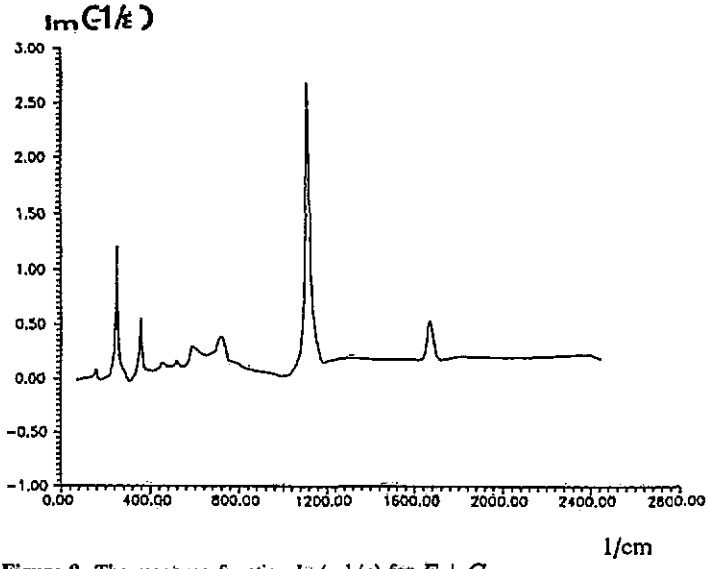

Figure 8. The response function $\mathrm{Im}(-1/\epsilon)$ for $E \perp C$.

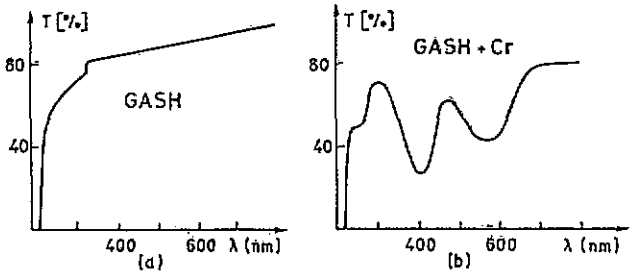

Figure 9. Room temperature transmission diagrams of (*a*) GASH and (*b*) GASH sample doped with Cr, respectively, for $E \parallel C$.

Table 3. Indices of refraction of GASH and G(Al, Cr)SH for $E \parallel C$ (n_e) and $E \perp C$ (n_w) and its differences ($N_w - n_e$).

	GASH	G(Al, Cr)SH
n_e ($E \parallel C$)	1.442 ± 0.001	1.444 ± 0.001
n_w ($E \perp C$)	1.531 ± 0.001	1.530 ± 0.001
$n_w - n_e$	0.089	0.096

Both our lattice parameters (given in table 1) for the hexagonal unit cell were slightly lower than values given in the literature [1]. This difference can be attributed to the approximately five times smaller number of Bragg reflections used by Schein *et al* [1].

Moreover, complete reflectivity experimental results for GASH in both infrared ranges are given here for the first time. As far as we know only preliminary work has been published concerning the infrared properties of GASH, over ten years ago [4], and only three oscillators were observed for each direction ($E \parallel C$ and $E \perp C$), and the oscillators were rather blurred. The reflectivity results obtained in this work can therefore only be compared with our experimental data for refraction indices. Our values for dielectric permittivity at the frequency higher than the infrared range were 1.7 and 1.8 for $E \parallel C$ and $E \perp C$, respectively. These data are not in very good agreement with the squared results of the

refraction indices for $E \parallel C$ and $E \perp C$, which were 2.08 and 2.34 respectively. Here one should still take into account that the value of dielectric permittivity should decrease between the infrared and visible range. It is more interesting that the deduced values of low frequency dielectric permittivity were very different for $E \parallel C$ and $E \perp C$ i.e. it increased from 5.8 (for $E \parallel C$) to about 21.5 (for $E \perp C$). Nevertheless, it should be remembered that the samples for the $E \parallel C$ direction had inferior surfaces compared to the samples for the $E \perp C$ direction. The measured intensity of the reflectivity was smaller and that produced smaller values for dielectric permittivities.

The positions of longitudinal and transversal modes obtained using both Kramers–Krönig analysis and the four-parameter method differed for some oscillators, as can be seen by comparing tables 2(a) and 2(b). With the Kramers–Krönig method our experimental results were in good agreement with the theoretical curves. Our experimental results were also numerically analysed using a four-parameter model introduced by Gervais and Piriou [5]. The factorized form of the dielectric function is:

$$\epsilon = \epsilon_1 \pm i\epsilon_2 = \epsilon_\infty \prod_i \frac{\omega_{iLO}^2 - \omega^2 + i\gamma_{iLO}\omega}{\omega_{iTO}^2 - \omega^2 + i\gamma_{iTO}\omega}. \tag{2}$$

Table 2(b) displays the oscillator parameters and dielectric permittivity for the two polarization directions. They were deduced from a least-squares computer fit to the experimental reflectivity data where γ_{iLO} and γ_{iTO} represent the damping factor of transversal and longitudinal optical frequencies for each oscillator.

These results are in reasonable agreement with the Kramers–Krönig analysis given in table 2(a). Nevertheless when the four-parameter method was used for numerical analysis the best fit to the experimental results was poorer than for the Kramers–Krönig analysis. We have been using Roessler's method [6] where no assumptions are needed concerning the behaviour of the reflectance data outside the experimental range, and no extrapolations of data are required. The error in integration gradually builds up in Kramers–Krönig analysis but the uncertainties are much smaller compared with our experimental results.

The purpose of giving the results using a four-parameter model was to find values of damping factors of transversal and longitudinal optical frequencies, and oscillator energies for each oscillator. For oscillators which have damping factors wider than 50 cm^{-1} the splitting of these bands into two or more bands might be expected if the measurements could be done at liquid helium temperature. Then one might expect to observe many more very weak, 'not visible', ionic oscillators at room temperature. Tables 2(a) and 2(b) show that the positions of longitudinal frequencies for $E \parallel C$ differ by less than 5 cm^{-1} for 5 oscillators (1, 2, 3, 4, 9), but for $E \perp C$ this is the case for 9 oscillators (1, 2, 3, 4, 5, 7, 8, 10 and 12). With the Kramers–Krönig method the experimental and theoretical results are in better agreement than for the four-parameter model, so the first method of analysis is more reliable in our case, with more than 10 oscillators. However the four-parameter model gives more information about the character of the ionic resonance. It is necessary to know this for calculation of the oscillator energy and the effective Szigeti charge for both directions $E \parallel C$ and $E \perp C$.

The oscillator energy E_{osc} was also calculated for each oscillator using the following equation:

$$E_{osc} = \epsilon_{2max}\gamma_{TO}\omega_{TO}. \tag{3}$$

The ratio between the oscillator energy with the highest and lowest energy for $E \parallel C$ (E_{osc8}/E_{osc3}) $\simeq$ 16.6 and for $E \perp C$ (E_{osc11}/E_{osc1}) $\simeq$ 12.2. It may be expected that if the

measurements were made at liquid helium temperature the oscillators with very high energy would be observed as two or more individual oscillators.

A better idea of the accuracy of each method can be gained when the results are compared using the Lyddane–Sachs–Teller relation in the general form:

$$\prod_i (\omega_{LOi} - \omega_{TOi})^2 = \epsilon_0/\epsilon_\infty. \tag{4}$$

In our case, the values of the left and right hand sides of this equation are 14.00 and 11.94 respectively, for $\boldsymbol{E} \perp \boldsymbol{C}$ using the results for ω_{LO} and ω_{TO} obtained with the Kramers–Krönig method. In the case of the $\boldsymbol{E} \parallel \boldsymbol{C}$ direction the difference between the left and right sides was much larger, the values being 10.96 and 3.41 respectively. The results obtained with the fitting procedure (using the four-parameter method) differed more. For $\boldsymbol{E} \perp \boldsymbol{C}$ the left and right side of equation (4) were 12.24 and 8.08, respectively, but for $\boldsymbol{E} \parallel \boldsymbol{C}$ the values were 12.37 and only 2.29, respectively. The main reasons for these differences is probably the smaller size and inferior quality of the (100) surfaces compared to the (001) surfaces.

Using the transmission results, given in figures 9(a) and 9(b), the energy gap of pure GASH was calculated to be 5.64 eV. The samples doped with Cr (which were slightly blue) had three relatively wide energy bands in the forbidden energy zone below the conduction zone at the distances of about 2.6 eV, 3.0 eV and 4.8 eV.

4. Conclusion

The lattice parameters for single crystals of GASH were determined with better accuracy than had been obtained previously. For the first time complete infrared reflectivity spectra have been measured and analysed for GASH single crystals in two directions ($\boldsymbol{E} \parallel \boldsymbol{C}$ and $\boldsymbol{E} \perp \boldsymbol{C}$). The indices of refraction were measured using a classical polarized microscope (Reichert) and the immersion method with Cargille liquid. The data obtained were slightly lower than those from the numerical analysis of reflectivity measurements in the infrared and far-infrared ranges.

Using transmission measurements in the absorption edge it was shown that the values of the energy gap for GASH and GASH doped with Cr were very similar. Moreover, three wide energy bands were observed below the conduction energy zone (at distances of about 2.6 eV, 3.0 eV and 4.8 eV).

Acknowledgment

The valuable help of Mr J Cvetic in computing the data is gratefully acknowledged.

References

[1] Schein B J B, Lingafelter E C and Stewart J M 1967 *J. Chem. Phys.* **47** 5183–9
[2] Schein B J B and Lingafelter E C 1967 *J. Chem. Phys.* **47** 5190–4
[3] Adams D M and Newton D C 1970 *'Tables for Factor Group Analysis'* (New York: Beckman RIIC)
[4] Nikolic P M, Roys W B, Todorovic D, Rakovic D and Grbic R 1980 *Fizika Suppl.* 1 **12** 165–8
[5] Gervais F and Piriou B 1974 *Phys. Rev.* B **10** 1642
[6] Roessler D M 1965 *Br. J. Appl. Phys.* **16** 1119